Article

Single-Label Kinase and Phosphatase Assays for Tyrosine Phosphorylation Using Nanosecond Time-Resolved Fluorescence Detection

Harekrushna Sahoo, Andreas Hennig, Mara Florea, Doris Roth, Thilo Enderle, and Werner M. Nau

J. Am. Chem. Soc., **2007**, 129 (51), 15927-15934 • DOI: 10.1021/ja074975w

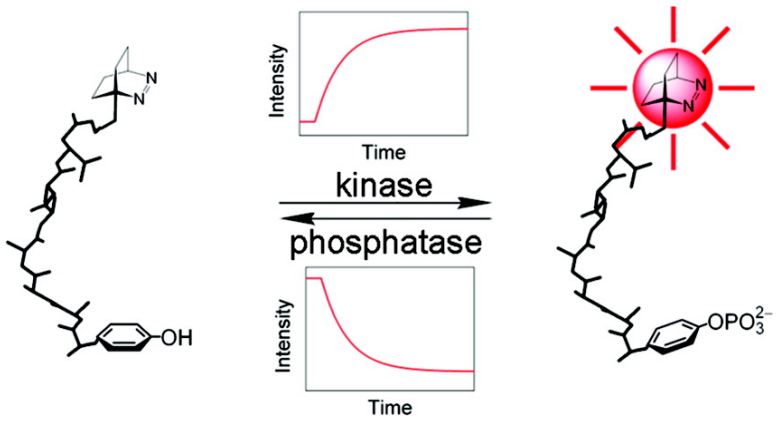

More About This Article

Additional resources and features associated with this article are available within the HTML version:

- Supporting Information
- Access to high resolution figures
- Links to articles and content related to this article
- Copyright permission to reproduce figures and/or text from this article

View the Full Text HTML

J|A|C|S
ARTICLES
Published on Web 11/29/2007

Single-Label Kinase and Phosphatase Assays for Tyrosine Phosphorylation Using Nanosecond Time-Resolved Fluorescence Detection

Harekrushna Sahoo,[†] Andreas Hennig,[†] Mara Florea,[†] Doris Roth,[‡] Thilo Enderle,[‡] and Werner M. Nau*[,†]

Contribution from the School of Engineering and Science, Jacobs University Bremen, Campus Ring 1, D-28759 Bremen, Germany, and F. Hoffmann-La Roche AG, Grenzacherstrasse 124, CH-4070 Basel, Switzerland

Received July 5, 2007; E-mail: w.nau@jacobs-university.de

Abstract: The collision-induced fluorescence quenching of a 2,3-diazabicyclo[2.2.2]oct-2-ene-labeled asparagine (Dbo) by hydrogen atom abstraction from the tyrosine residue in peptide substrates was introduced as a single-labeling strategy to assay the activity of tyrosine kinases and phosphatases. The assays were tested for 12 different combinations of Dbo-labeled substrates and with the enzymes $p60^{c-Src}$ Src kinase, EGFR kinase, YOP protein tyrosine phosphatase, as well as acid and alkaline phosphatases, thereby demonstrating a broad application potential. The steady-state fluorescence changed by a factor of up to 7 in the course of the enzymatic reaction, which allowed for a sufficient sensitivity of continuous monitoring in steady-state experiments. The fluorescence lifetimes (and intensities) were found to be rather constant for the phosphotyrosine peptides (ca. 300 ns in aerated water), while those of the unphosphorylated peptides were as short as 40 ns (at pH 7) and 7 ns (at pH 13) as a result of intramolecular quenching. Owing to the exceptionally long fluorescence lifetime of Dbo, the assays were alternatively performed by using nanosecond time-resolved fluorescence (Nano-TRF) detection, which leads to an improved discrimination of background fluorescence and an increased sensitivity. The potential for inhibitor screening was demonstrated through the inhibition of acid and alkaline phosphatases by molybdate.

Introduction

One of the most important regulatory mechanisms of biological signal transduction is the phosphorylation and dephosphorylation of tyrosine residues in proteins catalyzed by tyrosine kinases and phosphatases.[1,2] These enzymes play a key role in numerous diseases, such as pathogenic infections[3,4] or cancer.[5,6] In order to identify specific inhibitors and activators as potential lead structures for new drugs,[7] convenient and cost-effective kinase and phosphatase assays are required in pharmaceutical industrial drug discovery as well as in fundamental enzymological research. While several radioimmunoassays[8] as well as laborious electrophoretic[9] or chromatographic[10] assays have been developed, homogeneous fluorescence-based assays are very attractive due to their high sensitivity, short detection times, and their possibility for an easy scale-up to high-throughput screening (HTS) format. However, the modulation of the fluorescence, i.e., the translation of the phosphorylation into a decrease or an increase of fluorescence, presents a major obstacle in the design of fluorescence-based phosphorylation assays, and requires generally the use of expensive antibodies,[11,12] phosphate binding proteins[13] or biopolymers,[14] strategies involving metal particles,[15] or metal-ion chelating sites.[16]

2,3-diazabicyclo[2.2.2]oct-2-ene
(DBO)

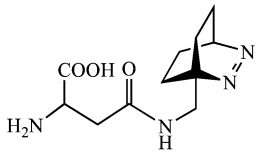

DBO-labeled asparagine
(Dbo)

[†] Jacobs University.
[‡] F. Hoffmann-La Roche AG.

(1) Hubbard, S. R.; Till, J. H. *Annu. Rev. Biochem.* **2000**, *69*, 373−398.
(2) Adams, J. A. *Chem. Rev.* **2001**, *101*, 2271−2290.
(3) Manger, M.; Scheck, M.; Prinz, H.; von Kries, J. P.; Langer, T.; Saxena, K.; Schwalbe, H.; Fürstner, A.; Rademann, J.; Waldmann, H. *ChemBioChem* **2005**, *6*, 1749−1753.
(4) McCain, D. F.; Grzyska, P. K.; Wu, L.; Hengge, A. C.; Zhang, Z.-Y. *Biochemistry* **2004**, *43*, 8256−8264.
(5) Johnson, L. N.; Lewis, R. J. *Chem. Rev.* **2001**, *101*, 2209−2242.
(6) van der Geer, P. V.; Hunter, T.; Lindberg, R. A. *Annu. Rev. Cell Biol.* **1994**, *10*, 251−337.
(7) von Ahsen, O.; Bömer, U. *ChemBioChem* **2005**, *6*, 481−490.
(8) Mallari, R.; Swearingen, E.; Liu, W.; Ow, A.; Young, S. W.; Huang, S.-G. *J. Biomol. Screening* **2003**, *8*, 198−204.
(9) Hunter, T. *J. Biol. Chem.* **1982**, *257*, 4843−4848.
(10) Budde, R. J. A.; McMurray, J. S.; Tinker, D. A. *Anal. Biochem.* **1992**, *200*, 347−351.
(11) Karvinen, J.; Laitala, V.; Mäkinen, M.-L.; Mulari, O.; Tamminen, J.; Hermonen, J.; Hurskainen, P.; Hemmilä, I. *Anal. Chem.* **2004**, *76*, 1429−1436.
(12) Parker, G. J.; Law, T. L.; Lenoch, F. J.; Bolger, R. E. *J. Biomol. Screening* **2000**, *5*, 77−88.
(13) Wang, Q.; Lawrence, D. S. *J. Am. Chem. Soc.* **2005**, *127*, 7684−7685.
(14) Simeonov, A.; Bi, X.; Nikiforov, T. T. *Anal. Biochem.* **2002**, *304*, 193−199.
(15) Wang, Z.; Lévy, R.; Fernig, D. G.; Brust, M. *J. Am. Chem. Soc.* **2006**, *128*, 2214−2215.
(16) Shults, M. D.; Imperiali, B. *J. Am. Chem. Soc.* **2003**, *125*, 14248−14249.

Scheme 1

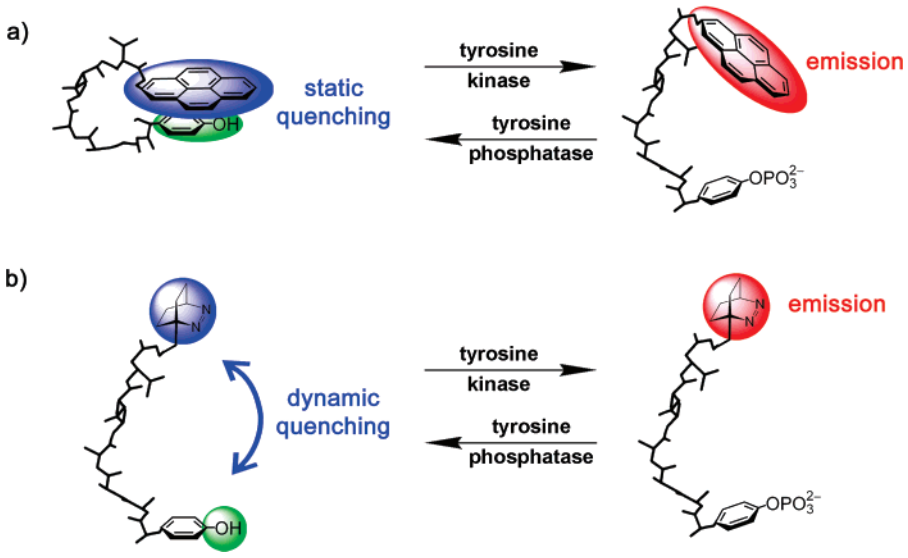

Very recently, Lawrence and co-workers reported an elegant single-labeling approach to assay tyrosine kinases using originally pyrene (Pyr) and also other dyes,[17−19] which show a differential propensity to form nonfluorescent intramolecular ground-state complexes with Tyr and pTyr residues and thereby variations in static quenching (Scheme 1a). Herein, we report our results on an alternative single-label assay to follow Tyr phosphorylation (kinases) and dephosphorylation (phosphatases), which is based on the dynamic fluorescence quenching of the fluorescent amino acid Dbo (Scheme 1b), an asparagine labeled with the 2,3-diazabicyclo[2.2.2]oct-2-ene (DBO) azo-chromophore.[20] Mechanistically, Dbo undergoes efficient intrachain collision-induced quenching by Tyr,[20,21] but not with pTyr. The resulting Dbo/Tyr assays are complementary to the recently reported Pyr/Tyr assays. In particular, we employ a small hydrophilic fluorophore, which is accessible to nanosecond time-resolved detection (Nano-TRF). Nano-TRF is an attractive method for efficient background subtraction, which we have recently established for protease assays.[22,23]

Experimental Section

Materials. Fmoc-protected Dbo (available as Puretime325 dye from Assaymetrics, Cardiff, U.K.) was synthesized according to the literature[20] and introduced into the peptide substrates by solid-phase synthesis (Biosyntan, Berlin); the purity of the peptides was >95%. $MgCl_2$, $MnCl_2$, EGTA, NaOAc, and Tris-HCl were purchased from Fluka or Sigma-Aldrich in highest commercial purity; glycine was from ICN Biomedicals.

Kinase Assays. The tyrosine kinase assays were performed in 100 mM Tris-HCl buffer (pH 7.2), containing 1.5 mM $MgCl_2$, 0.5 mM $MnCl_2$, and 0.5 mM EGTA. Peptide concentrations were determined UV spectrophotometrically (Varian Cary 4000) by using the molar extinction coefficient of tyrosine ($\epsilon_{275} = 1400\ cm^{-1}\ M^{-1}$).[24] Phosphorylation was initiated by adding 10 μL of Src kinase ($p60^{c-Src}$ from Proqinase, Germany, activity 142 pmol $\mu g^{-1}\ min^{-1}$ for the substrate poly(Glu, Tyr) in the ratio of 4:1) or 10 μL of EGFR (Sigma-Aldrich, activity 5000−30000 units/$mg^{-1}\ min^{-1}$ for the substrate poly(Glu, Tyr) in the ratio of 4:1) to a mixture of peptide substrate and 300 μM ATP in Tris buffer (10−50 μM of peptide, final assay volume 500 μL in semi-micro quartz glass cuvettes). The kinetic studies were carried out at 37.0 ± 0.1 °C using an external temperature controller (Peltier thermostat, Varian), and the fluorescence growth traces were recorded on a Varian Eclipse fluorometer ($\lambda_{exc} = 365$ nm and $\lambda_{obs} = 430$ nm).

Phosphatase Assays. YOP protein tyrosine phosphatase (truncated form, from *Escherichia coli*, in buffered aqueous glycerol solution, 30000 U/mg of protein), acid phosphatase (type I from wheat germ, 0.4 U/mg), and alkaline phosphatase (from *E. coli*, suspension in 2.5 M $(NH_4)_2SO_4$, 85.4 U/mg of protein) were obtained from Sigma-Aldrich. Peptide concentrations were determined by the molar extinction coefficient of phosphotyrosine ($\epsilon_{267} = 652\ cm^{-1}\ M^{-1}$).[25] The enzyme concentrations were determined either by using a defined volume of YOP phosphatase solution, or by using an extinction coefficient of $\epsilon_{278} = 1.26\ mg^{-1}\ cm^{-1}$ mL (for acid phosphatase), and $\epsilon_{278} = 0.72\ mg^{-1}\ cm^{-1}$ mL (for alkaline phosphatase).[26] Dephosphorylation was initiated by adding 42 μL of the YOP phosphatase solution, 50 μL of a 1 mg/mL acid phosphatase solution, or 50 μL of a 100 μg/mL alkaline phosphatase solution to a mixture of peptide substrate (25−50 μM, final assay volume 500 μL in semi-micro quartz glass cuvettes). The assays were conducted in 50 mM NaOAc buffer at pH 5.5 containing 0.5 mM EDTA adjusted to an ionic strength of 75 mM with NaCl (for YOP phosphatase),[27] 150 mM NaOAc buffer at pH 5.0 (for acid phosphatase), or in 130 mM glycine buffer with 8.3 mM $MgCl_2$ at pH 8.8 (for acid phosphatase). The temperature was maintained at 25.0 ± 0.1 °C as described above, except for YOP phosphatase (30.0 ± 0.1 °C), and the fluorescence decay traces were recorded on a Varian Eclipse fluorometer ($\lambda_{exc} = 365$ nm and $\lambda_{obs} = 450$ nm). The dephosphorylation by alkaline phosphatase was additionally monitored through the absorbance changes at 283 nm on a Varian Cary 4000 UV spectrophotometer.

(17) Wang, Q.; Cahill, S. M.; Blumenstein, M.; Lawrence, D. S. *J. Am. Chem. Soc.* **2006**, *128*, 1808−1809.
(18) Lawrence, D. S.; Wang, Q. *ChemBioChem* **2007**, *8*, 373−378.
(19) Wang, Q.; Dai, Z.; Cahill, S. M.; Blumenstein, M.; Lawrence, D. S. *J. Am. Chem. Soc.* **2006**, *128*, 14016−14017.
(20) Hudgins, R. R.; Huang, F.; Gramlich, G.; Nau, W. M. *J. Am. Chem. Soc.* **2002**, *124*, 556−564.
(21) Huang, F.; Hudgins, R. R.; Nau, W. M. *J. Am. Chem. Soc.* **2004**, *126*, 16665−16675.
(22) Hennig, A.; Roth, D.; Enderle, T.; Nau, W. M. *ChemBioChem* **2006**, *7*, 733−737.
(23) Hennig, A.; Florea, M.; Roth, D.; Enderle, T.; Nau, W. M. *Anal. Biochem.* **2007**, *360*, 255−265.
(24) Du, H.; Fuh, R.-C. A.; Li, J.; Corkan, L. A.; Lindsey, J. S. *Photochem. Photobiol.* **1998**, *68*, 141−142.
(25) Cousins-Wasti, R. C.; Ingraham, R. H.; Morelock, M. M.; Grygon, C. A. *Biochemistry* **1996**, *35*, 16746−16752.
(26) Anderson, R. A.; Bosron, W. F.; Kennedy, F. S.; Vallee, B. L. *Proc. Natl. Acad. Sci. U.S.A.* **1975**, *72*, 2989−2993.
(27) Zhang, Z.-Y.; Clemens, J. C.; Schubert, H. L.; Stuckey, J. A.; Fischer, M. W. F.; Hume, D. M.; Saper, M. A.; Dixon, J. E. *J. Biol. Chem.* **1992**, *267*, 23759−23766.

Time-Resolved Fluorescence Spectroscopy. Fluorescence lifetimes were recorded at $\lambda_{obs} = 450$ nm on a time-correlated single-photon counting (TCSPC) fluorometer (FLS 920, Edinburgh Instruments) by using 50-ps pulses from a PicoQuant diode laser LDH-P-C 375 ($\lambda_{exc} = 373$ nm, $\lambda_{obs} = 450$ nm, fwhm ca. 50 ps) for excitation. The lifetimes were analyzed with the instrument-specific software by means of a monoexponential or biexponential decay function (to account for short-lived impurities or scattered light) and judged on the basis of a reduced χ^2 around 1.0 and a random distribution of the weighted residuals around zero. Nanosecond time-resolved fluorescence assays (final assay volume was 50 μL) were carried out in black 384-well microplates (Corning NBS) with an LF 402 NanoScan FI microplate reader (IOM, Berlin, Germany). As an instrumental modification, an external nitrogen laser (MNL 200, Laser Technik Berlin, Germany) was coupled by optical fibers to a dye laser module, which provided an excitation wavelength of $\lambda_{exc} = 365$ nm. The experiments were performed at ambient temperature (25 °C) or at 40 °C.

Results and Discussion

DBO has been subject to extensive photophysical investigations,[28−37] and has recently found diverse applications in supramolecular[37−45] and biomolecular chemistry,[20,21,29,35,36,40,43−57] including its use in peptides[21−23,32,38,46−53] and enzyme assays.[22,23,48,52,54] The DBO chromophore stands alone due to its exceedingly long fluorescence lifetime of up to 1 μs in the gas phase and 320 ns in aerated water,[23,30,33,38,48] which enables the efficient suppression of background fluorescence[22] and an increased differentiation of product vs substrate by Nano-TRF detection.[23] In essence, the fluorescence can be measured after a sufficiently long time delay in the nanosecond range, e.g., after 150 or 500 ns. At this delay time, all background fluorescence (which is much shorter lived) has already decayed, while the long-lived fluorescence of DBO can still be reliably detected. In the case of protease assays,[22,23,52] we used Dbo-labeled substrates, which contained either Trp and Tyr as intramolecular quencher; the protease cleaved off probe or quencher, which led to a readily detectable fluorescence enhancement. Our conceptual approach to tyrosine kinases and phosphatases, which is shown in Scheme 1b, is based on the selective fluorescence quenching of Tyr; i.e., pTyr does not quench DBO fluorescence.

Table 1. Fluorescence Lifetimes[a] of the Unphosphorylated (**1**−**3**) and Phosphorylated (**p1**−**p3**) Model Peptides

peptide	sequence	H_2O (pH 7)	H_2O (pH 13)	D_2O (pD 7.4)
1	H-Y-Dbo-OH	80	6.7	145
p1	H-pY-Dbo-OH	360	285	530
2	H-AEYAARG-Dbo-OH	74	26	150
p2	H-AEpYAARG-Dbo-OH	290	250	410
3	H-Dbo-AEEEIYGE-OH	110 (80) [b]	58	180
p3	H-Dbo-AEEEIpYGE-OH	305 (263) [b]	310	430

[a] At 25 °C; 5% error. [b] Values in parentheses were measured at 40 °C.

Photophysical Characterization of Tyrosine and Phosphotyrosine Peptides. Previous studies on the fluorescence quenching of the parent chromophore DBO by amino acids have shown that Tyr acts as an efficient fluorescence quencher ($k_q = 5.6 \times 10^8$ M^{-1} s^{-1} in water at pH 7).[21] The mechanism of the collision-induced fluorescence quenching of DBO by phenols proceeds by a hydrogen atom transfer (which is aborted at a conical intersection),[29−31,55,56] as demonstrated through deuterium isotope effects,[20,21,35] and the observation of phenoxyl-type radicals.[35,57] Accordingly, the fluorescence of Dbo-labeled peptides containing Tyr is strongly quenched by intrachain collisions, the efficiency of which depends systematically on the distance between probe and quencher,[20,23,46−48] the amino acid sequence,[21,23,46,51] the temperature,[21,48] and the solvent viscosity.[20,21,46,51] The readily abstractable phenolic hydrogen of Tyr, which is responsible for the Dbo fluorescence quenching, is absent in pTyr. As a consequence, pTyr causes no significant, i.e., a more than 2 orders of magnitude lower, fluorescence quenching ($k_q \leq 5 \times 10^6$ M^{-1} s^{-1} in pH 7 phosphate buffer, this work). Thus, Dbo-labeled peptides containing pTyr should show the fluorescence characteristic for unquenched Dbo. According to the proposed assay principle in Scheme 1b, the action of a kinase is therefore expected to increase the fluorescence of the Dbo-labeled peptide, and that of a phosphatase is expected to decrease it.

The fluorescence lifetimes of Tyr vs pTyr containing model peptides (independently obtained by solid-phase synthesis) under different conditions are compared in Table 1; the relative lifetimes are expected to be proportional to the relative fluorescence intensities measured in conventional steady-state measurements. As expected from the intermolecular fluorescence quenching results, the fluorescence lifetime of the phosphorylated peptides (τ_{pY}) were invariably longer than those of the unphosphorylated (τ_Y) peptides, and the expected increase in fluorescence intensity in the course of an enzymatic reaction (estimated as τ_{pY}/τ_Y) was sufficiently large (3−40), to ensure sufficient sensitivity for the development of the respective kinase and phosphatase assays.

(28) Nau, W. M.; Greiner, G.; Wall, J.; Rau, H.; Olivucci, M.; Robb, M. A. *Angew. Chem., Int. Ed.* **1998**, *37*, 98−101.
(29) Nau, W. M.; Greiner, G.; Rau, H.; Olivucci, M.; Robb, M. A. *Ber. Bunsen-Ges. Phys. Chem.* **1998**, *102*, 486−492.
(30) Nau, W. M.; Greiner, G.; Rau, H.; Wall, J.; Olivucci, M.; Scaiano, J. C. *J. Phys. Chem. A* **1999**, *103*, 1579−1584.
(31) Sinicropi, A.; Pischel, U.; Basosi, R.; Nau, W. M.; Olivucci, M. *Angew. Chem., Int. Ed.* **2000**, *39*, 4582−4586.
(32) Nau, W. M.; Huang, F.; Wang, X.; Bakirci, H.; Gramlich, G.; Márquez, C. *Chimia* **2003**, *57*, 161−167.
(33) Mohanty, J.; Nau, W. M. *Photochem. Photobiol. Sci.* **2004**, *3*, 1026−1031.
(34) Nau, W. M.; Pischel, U. In *Organic Photochemistry and Photophysics*; Ramamurthy, V., Schanze, K. S., Eds.; CRC Press: 2006; Vol. 14, pp 75−129.
(35) Pischel, U.; Patra, D.; Koner, A. L.; Nau, W. M. *Photochem. Photobiol.* **2006**, *82*, 310−317.
(36) Koner, A. L.; Pischel, U.; Nau, W. M. *Org. Lett.* **2007**, *9*, 2899−2902.
(37) Hennig, A.; Schwarzlose, T.; Nau, W. M. *Arkivoc* **2007**, (viii) 341−357.
(38) Nau, W. M.; Wang, X. *ChemPhysChem* **2002**, *3*, 393−398.
(39) Márquez, C.; Pischel, U.; Nau, W. M. *Org. Lett.* **2003**, *5*, 3911−3914.
(40) Zhang, X.; Gramlich, G.; Wang, X.; Nau, W. M. *J. Am. Chem. Soc.* **2002**, *124*, 254−263.
(41) Bakirci, H.; Koner, A. L.; Nau, W. M. *Chem. Commun.* **2005**, 5411−5413.
(42) Bakirci, H.; Koner, A. L.; Nau, W. M. *J. Org. Chem.* **2005**, *70*, 9960−9966.
(43) Bakirci, H.; Nau, W. M. *Adv. Funct. Mater.* **2006**, *16*, 237−242.
(44) Bakirci, H.; Koner, A. L.; Schwarzlose, T.; Nau, W. M. *Chem. Eur. J.* **2006**, *12*, 4799−4807.
(45) Bakirci, H.; Koner, A. L.; Dickman, M. H.; Kortz, U.; Nau, W. M. *Angew. Chem., Int. Ed.* **2006**, *45*, 7400−7404.
(46) Huang, F.; Nau, W. M. *Angew. Chem., Int. Ed.* **2003**, *42*, 2269−2272.
(47) Huang, F.; Nau, W. M. *Res. Chem. Intermed.* **2005**, *31*, 717−726.
(48) Sahoo, H.; Hennig, A.; Nau, W. M. *Int. J. Photoenergy* **2006**, DOI:10.1155/IJP/2006/89638 (OPEN ACCESS).
(49) Sahoo, H.; Roccatano, D.; Zacharias, M.; Nau, W. M. *J. Am. Chem. Soc.* **2006**, *128*, 8118−8119.
(50) Sahoo, H.; Nau, W. M. *Indian J. Radiat. Res.* **2006**, *3*, 104−112.
(51) Sahoo, H.; Nau, W. M. *ChemBioChem* **2007**, *8*, 567−573.
(52) Hennig, A.; Ghale, G.; Nau, W. M. *Chem. Commun.* **2007**, 1614−1616.
(53) Sahoo, H.; Roccatano, D.; Hennig, A.; Nau, W. M. *J. Am. Chem. Soc.* **2007**, *129*, 9762−9772.
(54) Hennig, A.; Bakirci, H.; Nau, W. M. *Nat. Methods* **2007**, *4*, 629−632.
(55) Sinicropi, A.; Pogni, R.; Basosi, R.; Robb, M. A.; Gramlich, G.; Nau, W. M.; Olivucci, M. *Angew. Chem., Int. Ed.* **2001**, *40*, 4185−4189.
(56) Sinicropi, A.; Nau, W. M.; Olivucci, M. *Photochem. Photobiol. Sci.* **2002**, *1*, 537−546.
(57) Nau, W. M. *J. Am. Chem. Soc.* **1998**, *120*, 12614−12618.

The model dipeptide **1** with adjacent probe and quencher (no intervening amino acid) showed the largest difference (factor 4.5 in H_2O at pH 7) in fluorescence lifetimes, but the differentiation for peptide **2** (with four intervening amino acids) was also quite large (factor 3.9 in H_2O at pH 7), owing to the weak variations of the intrachain quenching rate for short peptides[20,47,48] and the presence of the highly flexible glycine.[20−23,46,48] Peptide **3**, with five intervening amino acids and one being a rigid isoleucine,[21,46] showed a slightly smaller differentiation between the phosphorylated and unphosphorylated peptide (factor 2.8 in H_2O at pH 7). The differentiation in fluorescence lifetimes (and intensities) increased significantly at alkaline pH, e.g., to a factor of 40 for peptide **1**, Table 1.[58] Thus, at pH 13, the fluorescence lifetimes of the phosphorylated peptides remained similar, around the 300-ns benchmark characteristic for the parent DBO, while those of the unphosphorylated peptides dropped quite steeply, owing to the deprotonation of Tyr ($pK_a = 10.1$).[59] The latter converts the phenol residue into a phenolate, which serves as an even more efficient quencher (with exciplex formation as presumed quenching mechanism).[20,21,31,60] Moreover, owing to the temperature dependence of intrachain fluorescence quenching,[21,48,61,62] the differentiation improved further at slightly elevated temperature (compare 40 °C values in parentheses in Table 1), which is frequently preferred for enzymatic reactions.

In addition, we determined the fluorescence lifetimes in D_2O (Table 1). The use of D_2O as an alternative solvent does not increase the differentiation in fluorescence lifetimes but increases the absolute fluorescence lifetimes (by nearly 50%), which can be used to further suppress fluorescent background when measuring in the Nano-TRF mode (see below). The longer fluorescence lifetimes are due to the reduced solvent-induced quenching in D_2O compared to that in H_2O.[21,29,30,48] The variations in fluorescence lifetimes in H_2O and D_2O can be further used to calculate the kinetic isotope effect (KIE) on the intrachain quenching rate constants according to eq 1,[28−30] where the fluorescence lifetimes of the phosphorylated peptides were taken as the respective "unquenched" lifetimes. The resulting values ranged from 1.8 to 2.3, which provides additional support for hydrogen atom abstraction as quenching mechanism in these peptides. The absolute KIE values are comparable to those previously observed for intermolecular quenching by Tyr.[20,21,35]

$$\mathrm{KIE} = k_q^{H_2O}/k_q^{D_2O} = \left(\frac{1}{\tau_Y^{H_2O}} - \frac{1}{\tau_{pY}^{H_2O}}\right)/\left(\frac{1}{\tau_Y^{D_2O}} - \frac{1}{\tau_{pY}^{D_2O}}\right) \quad (1)$$

Enzyme Selection and Assay Performance. With the effect of phosphorylation on the fluorescence at hand, we selected two kinases ($p60^{c-Src}$ Src and EGFR kinases) and three phosphatases (the specific YOP protein tyrosine phosphatase, and the nonspecific alkaline and acid phosphatases) to test the novel tyrosine phosphorylation assay system. The nonreceptor kinase $p60^{c-Src}$ is a member of the Src family of cytoplasmic nonreceptor protein tyrosine kinases. Its most important function comprises the phosphorylation of Tyr-527 at the C-terminal end of the Src protein that promotes the association of the tail region with the SH2 domain and transmits signals involved in cell movement and proliferation.[63,64] The transmembrane receptor kinase EGFR (epidermal growth receptor factor) is a member of the ErbB family receptors. EGFR activation triggers numerous downstream signaling pathways such as mitogenesis and apoptosis, enhanced cell motility, protein secretion, cell differentiation, and upregulated EGFR signaling is correlated to a wide variety of tumors including their progression, invasion, and metastasis.[64−66]

Yersinia outer membrane protein (YOP) is the best-characterized protein tyrosine phosphatase and is an essential virulence determinant of *Yersinia pestis* (bubonic plague or Black Death).[4,27] Acid phosphatases from wheat germ are nonspecific enzymes acting as orthophosphoric monoester and pyrophosphate phosphohydrolases under acidic conditions.[67] They are responsible for the ATP and GTP depletion during free cell translation.[68,69] Alkaline phosphatase is a homodimeric protein with nonspecific phosphoesterase activity. In contrast to the YOP and acid phosphatase, the removal of the phosphate group by alkaline phosphatase takes place at an optimum alkaline pH. Alkaline phosphatase has been widely used as an antibody label in enzyme immunoassays capable of detecting primary analytes, for example drugs and pesticides such as cocaine,[70] digoxin,[71] and 2,4-dichlorophenoxyacetic acid.[72]

The fluorescence response of peptides **1**−**6** (Table 2) in steady-state experiments under the enzymatic reaction conditions (Figure 1) was consistent with expectations from the photophysical parameters determined for the model peptides **1**−**3** and **p1**−**p3** (Table 1). We observed a continuous increase upon addition of kinase and a continuous decrease upon addition of phosphatase (Figure 2).[73] At the selected enzyme and substrate concentrations (cf. Experimental Section), the reaction times ranged from less than 30 min (acid and alkaline phosphatase) up to several hours (kinases, YOP phosphatase). The results

(58) The use of strongly alkaline pH sacrifices the possibility for a continuous measurement, but the addition of base could be used to deliberately terminate the enzymatic reaction ("stopped assay") and offers a unique way to dramatically enhance the differentiation of substrate and product.
(59) Sjögren, H.; Ericsson, C. A.; Evenäs, J.; Ulvenlund, S. *Biophys. J.* **2005**, *89*, 4219−4233.
(60) Pischel, U.; Nau, W. M. *J. Am. Chem. Soc.* **2001**, *123*, 9727−9737.
(61) In contrast, for assays based on static fluorescence quenching (Scheme 1a), increased temperature should reduce the substrate/product differentiation, owing to the entropy loss accompanying probe/quencher aggregation.
(62) Roccatano, D.; Sahoo, H.; Zacharias, M.; Nau, W. M. *J. Phys. Chem. B* **2007**, *111*, 2639−2646.
(63) Haskell, M. D.; Slack, J. K.; Parsons, J. T.; Parsons, S. J. *Chem. Rev.* **2001**, *101*, 2425−2440.
(64) Thomas, S. M.; Brugge, J. S. *Annu. Rev. Cell Dev. Biol.* **1997**, *13*, 513−609.
(65) Wells, A. *Int. J. Biochem. Cell Biol.* **1999**, *31*, 637−643.
(66) Oda, K.; Matsuoka, Y.; Funahashi, A.; Kitano, H. *Mol. Syst. Biol.* **2005**, *1*, E1−E17.
(67) Verjee, Z. H. M. *Eur. J. Biochem.* **1969**, *9*, 439−444.
(68) Shen, X.-C.; Yao, S.-L.; Terada, S.; Nagamune, T.; Suzuki, E. *Biochem. Eng. J.* **1998**, *2*, 23−28.
(69) Kawarasaki, Y.; Nakano, H.; Yamane, T. *Plant Sci.* **1996**, *119*, 67−77.
(70) Eremenko, A. V.; Bauer, C. G.; Makower, A.; Kanne, B.; Baumgarten, H.; Scheller, F. W. *Anal. Chim. Acta* **1998**, *358*, 5−13.
(71) Nistor, C.; Emnéus, J. *Anal. Commun.* **1998**, *35*, 417−419.
(72) Bauer, C. G.; Eremenko, A. V.; Ehrentreich-Förster, E.; Bier, F. F.; Makower, A.; Halsall, H. B.; Heineman, W. R.; Scheller, F. W. *Anal. Chem.* **1996**, *68*, 2453−2458.
(73) In order to provide an independent quantitfication of the degree of conversion in the Dbo-based assays, we developped an independent UV assay, in which the dephosphorylation of peptide **p6** by alkaline phosphatase was directly monitored through the distinct changes in the UV spectra of the tyrosine residue. Accordingly, dephosphorylation converts a phosphotyrosine residue ($\lambda_{max} = 273$ nm, ϵ ca. 650 cm^{-1} M^{-1}, ref 25) to a tyrosine group ($\lambda_{max} = 276$ nm, ϵ ca. 1400 cm^{-1} M^{-1}, ref 24), which results in a characteristic bathochromic and hyperchromic shift of the tyrosine absorption band. The conversion time profile as obtained by monitoring the UV absorbance of tyrosine at 283 nm, where the absolute variations in absorbance were largest, was the same, within error, as that obtained by monitoring the fluorescence of Dbo at 450 nm, which confirmed that the fluorescence changes depend linearly on the degree of conversion.

Table 2. Fluorescence Lifetimes[a] of Peptides **1**−**6** before and after the Enzymatic Reaction with a Kinase or Phosphatase, Ratios of Fluorescence Lifetimes, and Steady-State Fluorescence Intensity Ratios

substrate		product		enzyme[b]	pH	τ_Y /ns	τ_{pY} /ns	τ_{pY}/τ_Y	I_{pY}/I_Y
Phosphorylation by Kinases at 37 °C									
2	H-AEYAARG-Dbo-OH	**p2**	H-AEpYAARG-Dbo-OH	Src	7.2	82	—[c]	—[c]	—[c]
				EGFR	7.2	82	290	3.5	2.0
3	H-Dbo-AEEEIYGE-OH	**p3**	H-Dbo-AEEEIpYGE-OH	Src	7.2	80	240	3.0	2.5
4	H-Dbo-AEEEIYGEFEAKKKK-NH_2	**p4**	H-Dbo-AEEEIpYGEFEAKKKK-NH_2	Src	7.2	100	230	2.3	2.2
5	H-Dbo-GEYGEF-NH_2	**p5**	H-Dbo-GEpYGEF-NH_2	Src	7.2	40	245	6.1	6.7
Dephosphorylation by Phosphatases at 25 °C									
p1	H-pY-Dbo-OH	**1**	H-Y-Dbo-OH	AcP	5.0	71	350	4.9	4.1
				AlkP	8.8	31	300	9.6	6.8
p2	H-AEpYAARG-Dbo-OH	**2**	H-AEYAARG-Dbo-OH	AcP	5.0	—[c]	285	—[c]	—[c]
				AlkP	8.8	68	295	4.3	2.6
				YOP[d]	5.5	70	285	4.1	1.5
p3	H-Dbo-AEEEIpYGE-OH	**3**	H-Dbo-AEEEIYGE-OH	AcP	5.0	100	365	3.6	2.0
				AlkP	8.8	120	310	2.6	2.0
p6	H-Dbo-EEEEpY-OH	**6**	H-Dbo-EEEEY-OH	AcP	5.0	69	300	4.3	2.8
				AlkP	8.8	86	290	3.4	2.1
				YOP[d]	5.5	70	300	4.3	2.5

[a] 10% error. [b] Abbreviations used: Src: $p60^{c-Src}$ kinase, EGFR: epidermal growth receptor factor, AcP: acid phosphatase, AlkP: alkaline phosphatase, and YOP: *Yersinia* outer membrane protein. [c] No enzymatic activity detected. [d] At 30 °C.

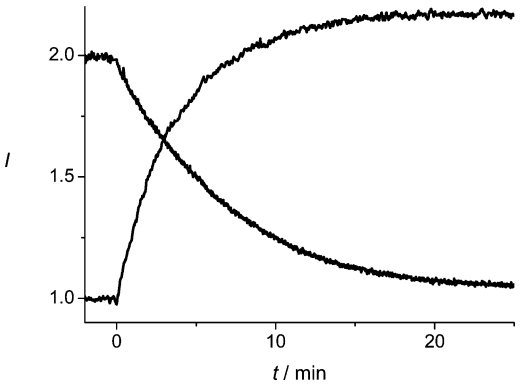

Figure 1. Traces of fluorescence intensity (λ_{exc} = 365 nm) upon addition of 50 μL of a 1 mg/mL solution of acid phosphatase to 50 μM H-Dbo-AEEEIpYGE-OH (**p3**) (decrease in fluorescence, λ_{obs} = 450 nm) and 10 μL of Src kinase to 10 μM H-Dbo-AEEEIYGEFEAKKKK-NH_2 (**4**) (increase in fluorescence, λ_{obs} = 430 nm).

confirmed the activity of the investigated enzymes and the feasibility of the assay principle in Scheme 1b. We also determined the fluorescence lifetimes before addition of enzyme and after the enzymatic reaction and observed an increase or decrease in fluorescence lifetimes in the actual reaction mixture (Table 2). As expected, the fluorescence lifetimes of the phosphorylated peptides were around 300 ns, with small variations with peptide structure, pH, temperature, etc. The intensity ratios in the steady-state (I_{pY}/I_Y) and time-resolved (τ_{pY}/τ_Y) measurements were also in satisfactory mutual agreement and compared well with the values determined for the model peptides in Table 1.

Assets of Assays Based on Single-Labeled Peptide Substrates. The Dbo/Tyr tyrosine kinase and phosphatase assays bypass the use of antibodies[11,12] or radiolabels[8] and operate without the necessity of additional incubation steps.[8,11,12] The response of the Dbo/Tyr fluorescence assay toward addition or removal of the phosphate group is immediate and direct. This allows continuous monitoring of the enzymatic reaction in homogeneous solution and convenient measurement of enzyme kinetics (see below).[73] The (weak) near-UV absorption of Dbo (λ_{max} ca. 365 nm, ϵ ca. 50 M^{-1} cm^{-1}) is compatible with common solid-state or LED laser excitation wavelengths (355 and 375 nm); the possibility for laser excitation is critical, along with the long fluorescence lifetime of Dbo, for the refined Nano-

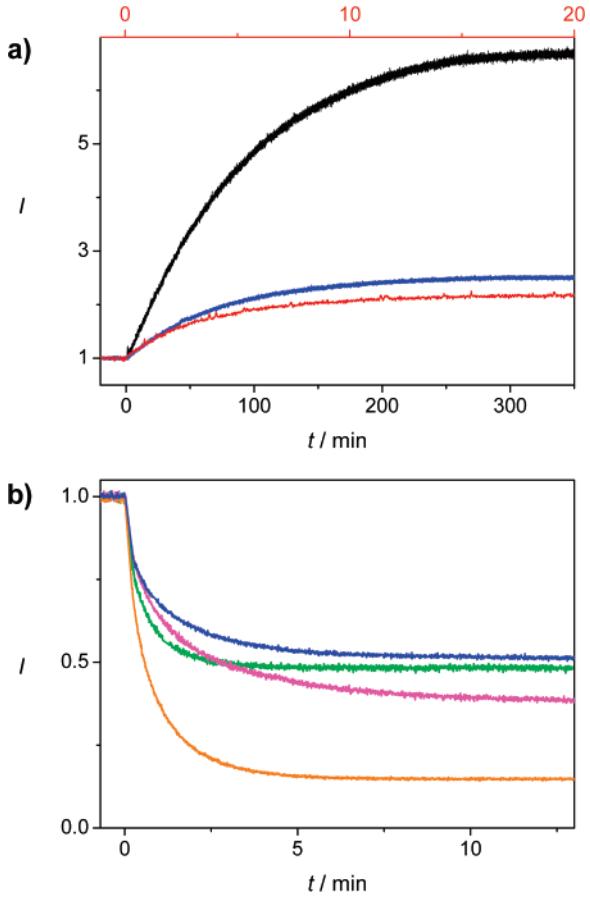

Figure 2. (a) Steady-state fluorescence intensity traces of Src kinase activity (normalized to the same initial fluorescence intensity). The assays were initiated by addition of 10 μL of Src kinase to 10 μM of peptide **3** (blue), **4** (red), and **5** (black), all at pH 7.2 at 37 °C with λ_{exc} = 365 nm and λ_{obs} = 430 nm. Note the much faster time scale (upper *x*-axis) for the enzymatic reaction of the most active peptide, **4**. (b) Steady-state fluorescence intensity traces of phosphatase activity (normalized to the same initial fluorescence intensity). The assays were initiated by addition of 50 μL of a 100 μg/mL solution of alkaline phosphatase to 50 μM of peptide **p1** (orange), **p2** (magenta), **p3** (blue), and **p6** (green), all at pH 8.8 at 25 °C with λ_{exc} = 365 nm and λ_{obs} = 450 nm.

-TRF detection and background suppression discussed below.

Instructive is also a comparison with the kinase assays developed by Lawrence and co-workers.[17−19] The original assay was based on the static fluorescence quenching of pyrene (Pyr) resulting from the hydrophobic association with tyrosine in equilibrium (Scheme 1a), as confirmed by the observation of NOE enhancements.[17] The driving force for this intrachain association decreases upon phosphorylation. Both fluorescence-based methods (Scheme 1) are based on single labeling (with either Pyr or Dbo) and exploit Tyr as an intrinsic contact quencher. However, in contrast to the dynamic (collision-induced) fluorescence quenching in the Dbo/Tyr system, the fluorescence quenching in the Pyr/Tyr system is thought to be static in nature. Phosphorylation of Tyr modulates the static quenching in the latter case and switches off the collision-induced quenching in the former case. The classification of the different quenching mechanisms and their merits in assay development have recently been outlined for protease assays.[23]

The two methods are highly complementary. Previous applications have illustrated, for example, the advantage of the small size (similar to Tyr) and hydrophilicity of the "noninvasive" Dbo fluorophore,[22,23,52] which broadens its application potential to assay quite different enzymes. Moreover, the fluorescent probe does not perturb the native conformation of peptides.[20,21,47,49−51,53] Although the use of Pyr is frequently prone to complications due to its higher hydrophobicity and larger size,[74−76] including a limited solubility of Pyr-appended peptides or occasionally inhibition of enzymatic activity, these problems were not encountered for the Pyr/Tyr kinase assays.[17] Moreover, Lawrence and co-workers have provided examples for the use in cellular fluorescence imaging,[18,19] applications for which the brightness of the Dbo chromophore would be presumably insufficient.

Optimization of Fluorescence Response and Determination of Enzyme Kinetic Parameters for Kinases. We selected the three peptides **3**−**5**, all of which derived from known recognition motifs of Src kinase,[77,78] to optimize the sensitivity, i.e., the fluorescence differentiation between product and substrate (I_{pY}/I_Y or τ_{pY}/τ_Y in Table 2), without sacrificing a high activity. Consequently, we performed the fluorescence assays in steady-state mode (Figures 1 and 2a) and compared the fluorescence lifetimes before and after phosphorylation to obtain the enhancement factors (Table 2). In peptides **3** and **4,** the fluorescent probe (Dbo) and the quencher (Tyr) are separated by the same number of amino acids (AEEEI), but peptide **4** has an extended carboxy-terminal tail (FEAKKKK-NH_2). From a fluorescence quenching point of view, the function of this tail may be that of a dangling chain end, which slows down intrachain collisions by effectively decreasing the diffusion coefficient, in this particular case for the quencher (Tyr).[50,79] Moreover, the C-terminal lysine residues in peptide **4** may undergo ion pairing with the *N*-terminal glutamates, which may result in a different structural preference, e.g. a more constrained conformation. In line with these presumptions, quenching is more efficient in the shorter peptide **3** (20% shorter fluorescence lifetime than **4**), and because the fluorescence lifetime of the *phosphorylated* peptide (**p3**) remains virtually constant (no significant quenching in either case), the product/substrate differentiation increases. Compared to peptides **3** and **4**, peptide **5** has a shorter "backbone" of only two amino acids (GE) and, more importantly, incorporates a highly flexible glycine residue. As we have documented in extensive mechanistic studies in the area of biopolymer dynamics,[20,21,32,38,46−48,50,80] the combination of the two factors (shorter separation and incorporation of a flexible amino acid) results in faster intrachain collision rates, which shortens the fluorescence lifetimes in peptide **5** and thereby leads to a very large enhancement factor of 6−7 (Table 2 and Figure 2a). In addition, it needs to be considered that the kinase assays were performed at a slightly elevated temperature (37 °C), which further increases the product/substrate differentiation compared to the ambient temperature data (Table 1). This is because the solvent viscosity decreases at higher temperature, which facilitates the dynamic collision-induced quenching.[21,48,61,62]

Table 3. Kinetic Parameters of the Investigated Peptides in Assays with Src Kinase[a]

peptide	sequence	K_M/ μM	v_{max}/ (μM/min)
3	H-Dbo-AEEEIYGE-OH	44	0.81
4	H-Dbo-AEEEIYGEFEAKKKK-NH_2	63	12.1
5	H-Dbo-GEYGEF-NH_2	103	1.0

[a] Obtained from Lineweaver−Burk plots, 10% error.

As can be seen from the foregoing, the fluorescence quenching mechanism between Dbo and Tyr is mechanistically well understood, which facilitates a rational design of the enzymatic substrate and adjustment of the temperature in order to achieve an optimal sensitivity. However, in the course of this design process, effects on the enzyme kinetic parameters require similar attention. Accordingly, we also determined for the Src kinase substrates the initial reaction rates from the normalized steady-state fluorescence traces at varying substrate concentrations. The double-reciprocal Lineweaver−Burk plots afforded the Michaelis−Menten constants K_M and the maximum rates v_{max} for the investigated substrate−enzyme combinations (Table 3). The K_M values were found to lie in the expected range of Src kinase substrates.[17,77,78,81] For example, peptide **4** has a K_M of 63 μM, whereas for the structurally related peptide H-AEEE-IYGEFEAKKKK-OH a K_M value of 33 μM has been reported.[77] The shorter peptide **5** shows a larger K_M value (103 μM), and the same trend applies for the related sequence Ac-FGEYGEF-NH_2, with a reported K_M of 479 μM.[78,81]

Peptide **4** contains an excellent recognition motif[77,78] and, accordingly, showed the highest activity. The carboxyl-terminally truncated peptide **3** displayed only a marginally improved fluorescence enhancement, but its phosphorylation

(74) Daugherty, D. L.; Gellman, S. H. *J. Am. Chem. Soc.* **1999**, *121*, 4325−4333.
(75) Soleilhac, J. M.; Cornille, F.; Martin, L.; Lenoir, C.; Fournié-Zaluski, M. C.; Roques, B. P. *Anal. Biochem.* **1996**, *241*, 120−127.
(76) Anne, C.; Cornille, F.; Lenoir, C.; Roques, B. P. *Anal. Biochem.* **2001**, *291*, 253−261.
(77) Songyang, Z.; Carraway, K. L., III; Eck, M. J.; Harrison, S. C.; Feldman, R. A.; Mohammadi, M.; Schlessinger, J.; Hubbard, S. R.; Smith, D. P.; Eng, C.; Lorenzo, M. J.; Ponder, B. A. J.; Mayer, B. J.; Cantley, L. C. *Nature* **1995**, *373*, 536−539.
(78) Edison, A. M.; Barker, S. C.; Kassel, D. B.; Luther, M. A.; Knight, W. B. *J. Biol. Chem.* **1995**, *270*, 27112−27115.
(79) Hyeon, C.; Thirumalai, D. *J. Chem. Phys.* **2006**, *124*, 104905 (1−14).
(80) Wang, X.; Nau, W. M. *J. Am. Chem. Soc.* **2004**, *126*, 808−813.
(81) A direct comparison of the v_{max} values was not attempted, because of the unknown absolute concentrations of active kinase in the commercial samples and because of the different mutants of the proteins used throughout the literature, which contain different domains of the human Src kinase. For example, the employed Proqinase sample was a GST fusion protein with a His-tag and a thrombin cleavage site.

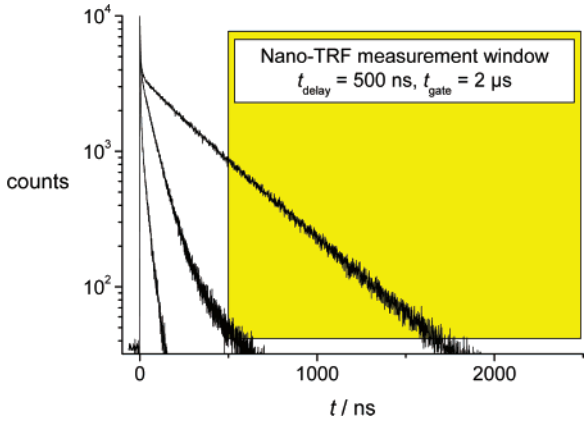

Figure 3. Comparison of the fluorescence lifetimes of phosphorylated and unphosphorylated peptides, obtained by single-photon counting. The long fluorescence lifetime (τ = 365 ns, peptide **p3** in 150 mM NaOAc buffer, pH 5.0) is representative for a phosphorylated peptide. The faster decay traces were obtained for peptide **1** after dephosphorylation with acid phosphatase (τ = 71 ns, in 150 mM NaOAc buffer, pH 5.0) and with alkaline phosphatase (τ = 31 ns, in 130 mM glycine buffer with 8.3 mM $MgCl_2$, pH 8.8). The spike at t = 0 ns stems from short-lived impurities in the assay mixtures.

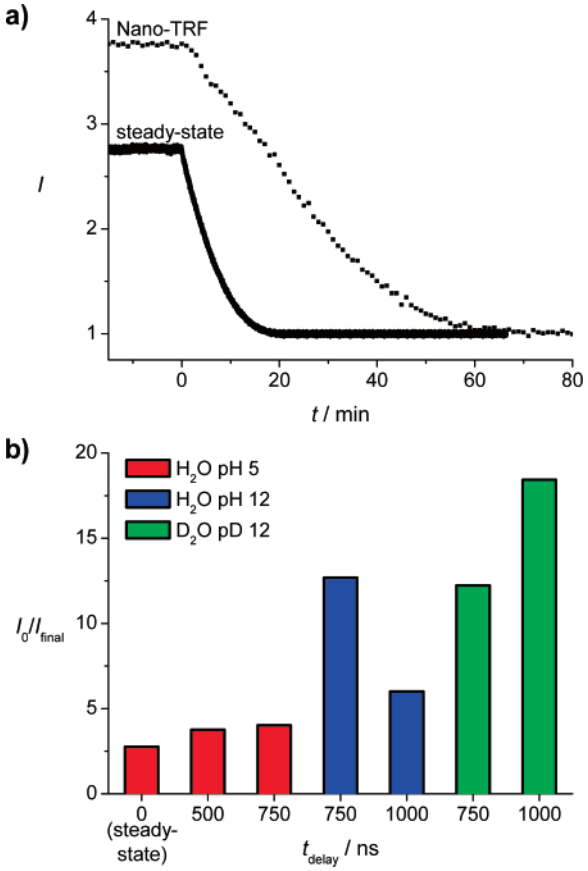

Figure 4. Optimization of a phosphatase assay by Nano-TRF detection (normalized to the same final fluorescence intensity). For the experiments H-Dbo-EEEEpY-OH was dephosphorylated by acid phosphatase at pH 5. (a) The steady-state trace refers to 30 μM peptide and 100 μg/mL acid phosphatase. The continuous Nano-TRF trace was recorded with 10 μM peptide and 20 μg/mL phosphatase (t_{delay} = 500 ns, t_{gate} = 2 μs). (b) Optimization of the substrate/product differentiation in a Nano-TRF measurement by addition of base (pH 12), by using D_2O (see text), and by varying the delay time (all measurements were recorded with 10 μM peptide); the differentiation in a steady-state experiment (corresponding to 0 delay time) is shown for comparison.

proceeded more slowly because it lacks the important phenylalanine in the Y+3 position.[77] The amino-terminal modification in peptide **5** presents a better alternative because this substrate displayed the highest fluorescence increase (factor 6−7) upon phosphorylation, and it had an acceptable activity as well. It should be noted that the Src kinase assay was also attempted with peptide **2**, for which the constant intensity of the fluorescence traces upon addition of enzyme signaled the lack of catalytic activity. Instead, the EGFR kinase favored peptide **2** as substrate and resulted in the expected increase in fluorescence. The combined examples for kinases and phosphatases establish Dbo/Tyr assays as a convenient tool to screen different substrates or enzymes for optimal activity by means of simple fluorescence experiments and select the substrate with highest sensitivity for a given enzyme.

Determination of Inhibition for Phosphatases. As previously demonstrated for Dbo-based protease assays,[23] the method can be implemented into HTS to search for inhibitors (or activators) of kinases and phosphatases. In HTS, the employed fluorescence detection, the direct monitoring in homogeneous solution without additional incubation steps, and the possibility to apply Nano-TRF are particularly advantageous. To provide an illustrative example for inhibitor testing, we determined the inhibitory effect of Na_2MoO_4 on the two nonspecific phosphatases. Molybdate is known as a general inhibitor of phosphatase activity with varying potency, depending on the exact type and source of the phosphatase.[67,82,83] We used the common[84] dose−response curve to determine the IC_{50}, which was 1.8 ± 0.3 mM and 0.09 ± 0.02 μM for alkaline (with peptide **p2** as substrate) and acid phosphatase (with peptide **p1**), respectively. This is consistent with the order of magnitude of reported inhibition constants of the two enzymes (K_i = 0.32 mM for alkaline phosphatase[83] and K_i = 0.07 μM for acid phosphatase[67]).

Optimizing the Substrate/Product Differentiation by Nano-TRF Detection. The most appealing asset of the Dbo-based assay is the possibility of using Nano-TRF detection, which is made possible by the exceedingly long fluorescence lifetime of Dbo. Figure 3 demonstrates the principle of Nano-TRF detection. In the case of a dephosphorylation reaction, i.e., in a phosphatase assay, the fluorescence intensity decreases (Figure 1), which is accompanied by a decrease in fluorescence lifetime. The ratio of fluorescence lifetimes is directly reflected in the ratio of the steady-state intensities before and after enzymatic conversion. However, in the Nano-TRF mode, the fluorescence is recorded after a certain delay time, t_{delay}, which efficiently suppresses any short-lived fluorescence as it unavoidably arises from impurities, library compounds in HTS, or sample container materials (see the initial spike in Figure 3).

The resulting desirable suppression of this background fluorescence is well-known from TRF assays with lanthanide chelates, which have lifetimes in the millisecond time range.[85−87] However, an added value of TRF detection is the possibility to increase the differentiation of substrate and product of an enzymatic reaction (Figure 4).[23,87] The experimental feasibility

(82) Pappas, P. W.; Leiby, D. A. *J. Cell. Biochem.* **1989**, *40*, 239−248.
(83) Stankiewicz, P. J.; Gresser, M. J. *Biochemistry* **1988**, *27*, 206−212.
(84) Copeland, R. A. *Anal. Biochem.* **2003**, *320*, 1−12.
(85) Hemmilä, I.; Webb, S. *Drug Discovery Today* **1997**, *2*, 373−381.
(86) Grepin, C.; Pernelle, C. *Drug Discovery Today* **2000**, *5*, 212−214.
(87) Johansson, M. K.; Cook, R. M.; Xu, J.; Raymond, K. N. *J. Am. Chem. Soc.* **2004**, *126*, 16451−16455.

of this improvement has only recently been demonstrated with lanthanide chelates for TRF assays,[87] and we have subsequently elaborated this method with a Nano-TRF protease assay.[23] Indeed, as can be seen from Figure 4a, the enhancement factor increases (from 2.8 to 3.8) in a phosphatase assay by changing from steady-state to Nano-TRF detection. In combination with the concomitant suppression of background fluorescence, the improved substrate/product differentiation can significantly improve the sensitivity of an assay, e.g., in HTS.[54] The time-dependent change of the Nano-TRF response in Figure 4a can be further used to follow the kinetics of the enzymatic reaction, but the temporal resolution is limited compared to steady-state detection, because each Nano-TRF intensity read-out requires the accumulation of several laser pulses.

By increasing the delay times of the Nano-TRF measurement window (Figure 3), it is possible to further optimize the differentiation of substrate and product fluorescence, as can be seen from the comparison of the steady-state intensity ("0 ns delay"), the Nano-TRF intensity for a 500 ns delay, and the Nano-TRF intensity for a 750 ns delay in Figure 4b. This characteristic dependence can be traced back to the nature of the exponential decay of the fluorescence intensity, i.e., the longer fluorescence lifetime contributes a higher fraction to the Nano-TRF intensity than the shorter lifetime at longer delay times.

To further improve the differentiation of substrate and product, we stopped the acid phosphatase assay by addition of base, which increased the pH from 5 to 12. Subsequently, we compared the Nano-TRF intensity of the product with that of the substrate. At the strongly alkaline pH, an increase in the differentiation of the fluorescence intensities of substrate and product was expected (see above and Table 2) and experimentally observed. For example, at a fixed 750 ns delay, the intensity ratio changed from 4 to 13 (Figure 4b). As can be seen from the comparison of the variation in delay times at pH 12 (from 750 to 1000 ns, Figure 4b), the differentiation decreased again at very long delays, where the signal intensity decreases and background fluorescence comes into play.[54] Measurement of the intensity ratio of substrate and product in D_2O (pD 12) instead of H_2O (pH 12) did not afford a significantly higher differentiation with a 750 ns delay time (Figure 4b). However, the longer fluorescence lifetime of the unquenched peptide allowed the application of longer delay times without sacrificing the detection limit (compare the Nano-TRF intensities for the 1000-ns delay in H_2O at pH 12 and D_2O at pD 12).

Conclusion

We have introduced a conceptually novel (dynamic fluorescence quenching) assay principle for kinases and phosphatases and a mechanistically novel (hydrogen transfer as quenching mechanism) assay principle for enzyme assays in general. The fluorescence lifetime of Dbo is sufficiently long to allow mutual diffusion to Tyr, which acts as a collision-induced fluorescence quencher, thereby shortening the fluorescence lifetime up to a factor of 7. By phosphorylation, it is possible to deactivate the quencher by removing the active abstractable hydrogen and thereby switch between a short-lived, weakly fluorescent state (the Dbo/Tyr peptide) and a long-lived, strongly fluorescent state (the Dbo/pTyr peptide), which can be conveniently utilized to follow the enzymatic activity of both kinases and phosphatases. A "fine-tuning" of the fluorescence response of the Dbo/Tyr assays can be achieved by varying the pH, the solvent, and the temperature. The sensitivity can be further enhanced by again making use of the long fluorescence lifetime of unquenched Dbo, which allows the application of a time-gated fluorescence detection in the form of the recently introduced Nano-TRF technique. The assay, which allows measurement in homogeneous solution with single-labeled peptides, is complementary to recently reported assays employing static fluorescence quenching and to those involving antibodies or radioactive labels.

Acknowledgment. This work was performed within a research collaboration of F. Hoffmann-La Roche. Financial support within the graduate program "Nanomolecular Science" at the Jacobs University Bremen, and by the Fonds der Chemischen Industrie, Frankfurt/Main, is gratefully acknowledged.

JA074975W